Journal of Power Sources 228 (2013) 104–111

Contents lists available at SciVerse ScienceDirect

Journal of Power Sources

journal homepage: www.elsevier.com/locate/jpowsour

Efficient air-breathing biocathodes for zinc/oxygen batteries

Adrianna Zloczewska, Martin Jönsson-Niedziolka*

Institute of Physical Chemistry, Polish Academy of Sciences, ul. Kasprzaka 44/52, 01-224 Warsaw, Poland

HIGHLIGHTS

- We created an efficient air-breathing biocathode for catalytic oxygen reduction.
- Toray paper functions both as electrode and gas permeable membrane.
- A catalytic oxygen reduction current of >2 mA cm^{-2} was measured.
- A Zn/O_2 biobattery was constructed with V_{OC} = 1.75 V.
- A power density of 5.25 mW cm^{-2} at 0.4 V was measured.

GRAPHICAL ABSTRACT

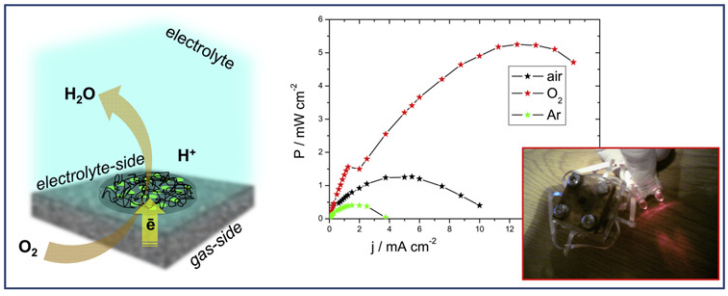

ARTICLE INFO

Article history:
Received 24 August 2012
Received in revised form
5 November 2012
Accepted 22 November 2012
Available online 29 November 2012

Keywords:
Hybrid biobattery
Bilirubin oxidase
Direct electron transfer
Air-breathing electrode
Zinc–oxygen battery

ABSTRACT

We present an efficient, easy to construct, air-breathing biocathode for dioxygen reduction using the enzyme bilirubin oxidase encapsulated in a silicate gel film on Toray paper. Functionalised single-walled carbon nanotubes were used for improving electron transfer between the enzyme and the Toray paper. A current density of 1.2 mA cm^{-2} was measured under air without any mediators. The biocathode was connected with a Nafion-covered Zn-anode to form a zinc–oxygen battery. The biobattery has an open circuit voltage of 1.75 V and gives a maximum power density of 5.25 mW cm^{-2} at ca 0.4 V, which is the best result published so far for such a device. The device was used to power a two-LED bicycle lamp.

© 2012 Elsevier B.V. All rights reserved.

1. Introduction

The last decade has seen an increasing interest in enzymatic biofuel cells. This is mostly directed towards the goal as future implantable power sources [1], but recently also other applications have been investigated [2]. In these kind of fuel cells enzymes are used as catalysts for the reactions occurring in the cell. The use of enzymatic catalysts is motivated by several advantages such as the high specificity, which decreases the risk of fuel cross over, the low overpotential and the ability of enzymes to work under mild conditions. Furthermore, enzymes can offer an economical and ecological alternative to expensive noble metal catalysts [3].

In a typical biofuel cell the cathode reaction would be the reduction of oxygen to balance the oxidation of the fuel at the anode. The most promising groups of enzymes for the construction of biocathodes are the members of the blue multicopper oxidases (BMCO) family. Apart from their primary functions the BMCO enzymes, such as bilirubin oxidase (BOD) or laccase can facilitate the catalytic reduction of dioxygen to water. They contain four copper ions which form two active centres; a T1 and a trinuclear T2/T3 cluster. The T1 is responsible for accepting electrons from the environment. The electrons are transported via a tripeptide His-Cys-His chain to the T2/T3 cluster where the dioxygen reduction takes place [4]. The reduction of each O_2 molecule requires four

* Corresponding author. Tel.: +48 22 343 3306; fax: +48 22 343 3333.
E-mail address: martinj@ichf.edu.pl (M. Jönsson-Niedziolka).

0378-7753/$ – see front matter © 2012 Elsevier B.V. All rights reserved.
http://dx.doi.org/10.1016/j.jpowsour.2012.11.081

electrons and only water molecules are formed as a product. No unwanted intermediates such as hydrogen peroxide are formed, which is a great advantage of BMCO catalysed reaction [5]. A second advantage is that some high-potential enzymes from BMCO can catalyse dioxygen reduction with a relatively low overpotential. A good example is BOD which has a redox potential of 0.69 V vs. NHE [6]. This is somewhat lower than the best laccases [7], but BOD generally has higher activity at neutral pH in comparison with other high-potential BMCO [8]. Taking into account the mentioned features and the fact that dioxygen is readily available in the subcutaneous liquids, one can understand that BOD has been seen as a very good candidate enzyme for the cathode of implantable biofuel cells. On the other hand, despite the ubiquitous nature of dioxygen there are still problems with transporting the gas to the BOD. Taking into account the values of diffusion coefficients of O_2 in water solutions and in the air, 2×10^{-5} cm^2 s^{-1} and 2×10^{-1} cm^2 s^{-1} respectively [9], as well as the relatively small amount of dioxygen that can be dissolved in water (ca 0.25 mmol dm^{-3} under air) it is obvious that the gas is transported much slower to biocathodes immersed in solution than to ones having a direct contact with the air. The main consequence of this phenomena is the limitation of the dioxygen reduction current by diffusion [10] for any relatively well designed biocathode. Several attempts to overcome this problem were described in the literature. One way is the use of forced convection, such as rotating disk electrodes [5] or microfluidic fuel cells [11,12]. Another way is the use of air-diffusion electrodes. The first reported biocathode which was using dioxygen directly from the air was floating on the surface of the electrolyte [13]. That floating electrode was made by drop-coating of a laccase/carbon material composite on a compressed hydrophobic carbon black pellet. A similar approach was later improved by Shleev et al. [14]. Later air-diffusion biocathodes with other BMCO, such as bilirubin oxidase and copper efflux oxidase were described [2,9,15–21]. These types of electrodes are composed of at least two layers: a diffusion and a catalytic layer. The first layer is kept in contact with the air and should be permeable for gas diffusion but act as a barrier for the electrolyte and the second layer is exposed to the electrolyte solution. An early air-breathing biocathode was developed by Nogala and co-workers using laccase immobilised in a carbon ceramic electrode in a glass tube immersed in electrolyte that was fed from the back with oxygen [15]. In this case the efficiency was low due to inefficient gas transport through the carbon paste. A very similar system, but with a more efficient carbon membrane (teflonized carbon black) was presented later by the Atanassov group [18]. In this case the maximum current density was close to 2 mA cm^{-2} in pure oxygen. Using the same cathode material in a different geometry, but with BOD instead of laccase, the efficiency was much lower [19]. Using functionalised teflonized carbon nanotube paper somewhat improved the BOD-cathodes [20]. A very high current cathode was presented by the Kano group using copper efflux oxidase [16]. However, the onset potential for biocatalysis using this enzyme is low, making it unsuitable for biofuel cells.

A few reports have combined air-breathing biocathodes with anodes to create functional biofuel cells or biobatteries. The Atanassov group combined their laccase electrode with malate dehydrogenase and alcohol dehydrogenase anodes creating a biofuel cell, albeit with relatively low power [17]. A higher power BOD-fuel cell was created by the Kano group [2]. Using glucose dehydrogenase (GDH) for the anode and a highly optimised gas flow cathode they managed to create a fuel cell that could drive a small RC car. To achieve this they employed a relatively large cell, with a moderate power density (1.45 mW cm^{-2}). Their system also suffers from the need to use of mediators for electron transport both at the anode and the cathode. Another interesting biofuel cell was recently published by Miyake et al. in which a highly efficient biocathode is coupled with a GDH anode and shown to work implanted in a grape as well as in a rabbit ear [9]. The highest power biofuel cell published with an air-breathing cathode was recently presented by Gellett and co-workers [21]. Using a laccase based biocathode with a platinum–ruthenium anode they construct H_2/O_2 and direct methanol fuel cells. The performance of the cells are excellent – the power density reaches 8.5 mW cm^{-2}. However, using a high current but relatively low potential laccase the Gellett-cell has its maximum power at just over 0.2 V cell potential. The construction of the cell also involves an ion exchange membrane, which makes the construction both more complicated and expensive than a simple membrane-less design.

Here we present an easy way of obtaining efficient air-diffusion biocathodes by the modification of Teflon treated Toray paper with functionalised carbon nanotubes (CNT) and bilirubin oxidase. These breathing electrodes demonstrate direct electron transfer and are successfully used in the construction of zinc/oxygen batteries which give the best power density and open circuit voltage reported so far. Moreover they can also be used in the fabrication of biofuel cells.

2. Experimental

2.1. Materials

Pyrene-1,3,6,8-tetrasulfonic acid tetrasodium salt hydrate (PTSA), and Nafion perfluorinated resin solution were purchased from Sigma–Aldrich. Single-walled carbon nanotubes (SWCNTs) were bought from Shenzhen Nano-tech Port Co. Ltd. Bilirubin oxidase (BOD) from *Myrothecium* sp. (EC 1.3.3.5) with an activity of 2.10 Umg^{-1} was donated by Amano Enzyme Inc. Toray Teflon Treated Carbon Paper TGP-H-090 was purchased from the Fuel Cell Store, Colorado. Methyltrimethoxysilane (MTMOS) from ABCR, zinc wire ($d = 0.250$ mm, purity 99.95%) from Goodfellow and zinc foil (0.25 mm, purity 99.98%) from Alfa Aesar. McIlvaine's buffer was prepared from Na_2HPO_4 (POCH S.A.) and citric acid (Chempur). Phosphate buffers were prepared from Na_2HPO_4 and NaH_2PO_4. Methanol, concentrated HCl and NaCl was purchased from Chempur. Deionised water obtained from an ELIX system (Millipore) was used for the preparation of all solutions.

2.2. Instrumentation and electrochemical measurements

All electrochemical experiments were carried out at ambient temperature (22–24 °C) with the potentiostats Autolab or μAutolab III (Metrohm Autolab). In the case the 3-electrode cell was used platinum wire or platinum net was used as counter electrode and $Ag|AgCl|KCl_{sat.(3M)}$ as reference electrode. The electrode made of modified Toray paper was used as working electrode (WE). Scanning electron microscope (SEM) images were taken using a FEI Nova NanoSEM system.

2.3. Modification of Toray paper

SWCNTs mixed with PTSA were sonicated with an ultrasonic finger (Bandelin electronics, Sonopuls HD2070, 40% amplitude) for 2 h. The suspension was left over night and then sonicated in a bath and filtered with at least 1 L of water. Then the functionalised tubes were dried and re-dispersed in water to a concentration of 2 $mgml^{-1}$. A similar system was previously examined for the preparation of biocathodes on ITO [22].

A sol–gel method, slightly modified from earlier descriptions [23,24], was used to encapsulate bilirubin oxidase on the Toray paper. For the sol preparation 375 μl of methanol, 250 μl of MTMOS

and 14 μl of concentrated HCl was sonicated for 15 min. Meanwhile 99 μl of 2 mg ml^{-1} BOD buffer solution was vortexed with 99 μl of PTSA–SWCNT suspension. Then 2 μl of the sol was added to the mix of enzyme and functionalised CNTs and vortexed for 3 min. 20 μl of this sol was drop-coated onto each electrode (within a circle with diameter 0.5 cm defined by adhesive tape, projected area = 0.2 cm^2) made of Toray paper and left for drying in room temperature for 17 h. The result is an electrode that is covered with a catalytic layer containing 19.8 μg of BOD from one side and can be exposed to the air from the other side (Fig. 1A). This electrode is called PTSA–SWCNT/BOD/$MTMOS_{gel}$. The electrodes were stored in a fridge at 4 °C until used.

For the preparation of the electrode without the enzyme 99 μl of buffer was used instead of BOD solution. For the preparation of the electrode without the functionalised carbon nanotubes 99 μl of water was used instead of the PTSA–SWCNT suspension.

2.4. Preparation of zinc anodes

Two similar types of the anode were prepared according to the paper by Shin et al. [25]. The first type was made by rolling ca 30 cm of zinc wire (surface area ca 1.5 cm^2) into a spiral. The wire was covered with a thin layer of Nafion by dipping it into 0.5% solution of Nafion in isopropanol and letting it dry. The Nafion-coated wire was then used as a working electrode in a three-electrode cell in 0.15 M NaCl and phosphate buffer (0.1 M, pH 7.0). Chronopotentiometry with the applied current density 13 μA cm^{-2} was performed for ca 16 h. Thanks to this modification of zinc in the presence of phosphate and chloride ions a layer of conductive hopeite was formed on the wire that protects the zinc anode from corrosion in contact with oxygen and enables stable operation of a zinc/oxygen battery also at low pH [25].

The second type of the anode was prepared by covering a piece of a zinc foil with a thin layer of Nafion and drying – in analogy to the preparation described above. In this case the area of the zinc foil anode was the same as the area of the biocathode, 0.2 cm^2. This type of the anode was used for the construction of the compact stack of air-breathing batteries whereas the first type was used in a in the Zn/O_2 test cell.

2.5. Assembly of the electrochemical test cell and the Zn/O_2 battery

A two compartment cell was made of plastic spectrometer cuvettes with holes (d = 0.5 cm) drilled with an electric drill. Between those compartments the working electrode was placed (Fig. 1). The modified Toray paper covered by the catalytic layer of silicate matrix ($MTMOS_{gel}$) encapsulating functionalised SWCNTs (black lines) and bilirubin oxidase (green spots in web version) (Fig. 1A) was used as WE. One of the cuvettes was filled with electrolyte and reference and counter electrodes were inserted. The side of the electrode with the catalytic layer exposed to the electrolyte will be referred to as the *electrolyte-side*. The other cuvette was flushed with Ar, oxygen or exposed to air. This way of constructing the cell let us to obtain a breathing electrode, which could be easily supplied with a selected type of a gas from the *gas-side*, via a gas nozzle. To prevent leakage a ringshaped silicone spacer was inserted on the electrolyte-side of the WE. Electric connection to the working electrode was made with a piece copper tape glued to the edge of the Toray paper. All parts were held together with a metal binder clip (Fig.1 in the supplementary material).

For the construction of the compact stack of batteries four air-breathing biocathodes and four anodes of the second type were put together as shown in Fig. 1D). The electrodes were separated by a PDMS mould with cylindrical holes filled with McIlvaine's buffer (cross section area 0.2 cm^2). All elements were held together firmly by metal plates and screws. Then the electrodes were connected in series by stripes of copper tape. This construction was done to generate higher voltage and power than those for a single battery cell.

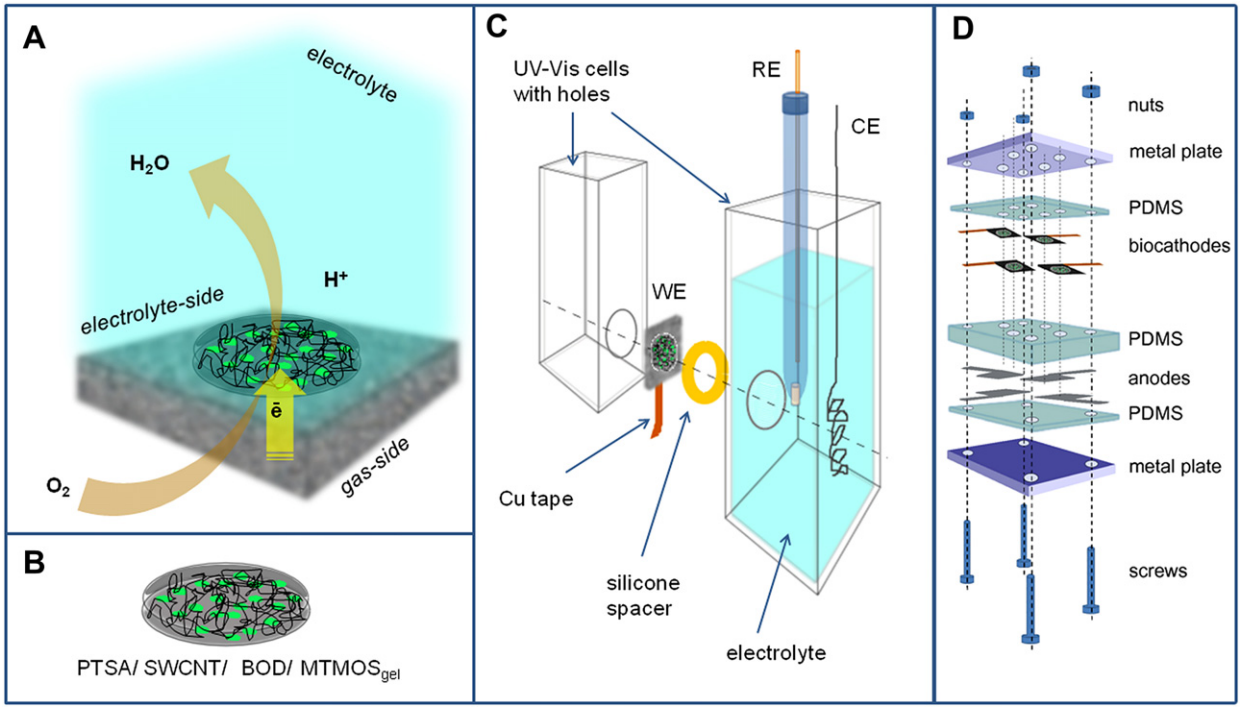

Fig. 1. Schematic visualisation of the air-breathing biocathode and biobattery assembly.

3. Results and discussion

3.1. Characterization of the air-breathing biocathode

Scanning electron microscopy was used to investigate the drop-coated composite material on the surface of the Toray paper (Fig. 2). Unmodified paper is shown in image A) where a network of randomly oriented carbon microfibres is visible. The same fibres are visible in the top right corner of the zoomed-out view in image C). The left part of image C) shows the layer of PTSA–SWCNT/BOD/$MTMOS_{gel}$ covering the Toray paper surface. A closer view of this layer (images B), D) and E)) shows that it has a porous structure, similar to SWCNT/$TMOS_{gel}$ electrodes on ITO [22], with enlarged surface area in comparison with the bare Toray paper. This kind of structure acts as a matrix encapsulating the enzyme on the surface of the electrode. The matrix is also sufficiently mechanically stable for the thin film of the composite material not to disintegrate during the measurements and after moving it out from the solution. Moreover the functionalised SWCNTs enable good, non-mediated electron transfer between the surface of the electrode and the active centre of the enzyme.

3.2. Efficient bioelectrocatalysis of the reduction of dioxygen

Cyclic voltammetry was carried out in a three-electrode cell (Fig. 1C) to show that the breathing biocathode is highly responsive to the type of gas introduced to the *gas-side*. The onset potential of the dioxygen reduction is ca 0.6 V vs. Ag|AgCl which is close to the formal potential of the T1 centre of BOD [6]. This high-potential is desirable for efficient cathodes in the biofuel cells.

As shown in Fig. 3 curve a), the current density of dioxygen reduction was the lowest when the *gas-side* was exposed to a stream of argon and the *electrolyte-side* contained deaerated buffer, ca 30 μA cm^{-2} at 0.1 V. Curve b) corresponds to the situation where the *gas-side* is exposed to argon but the *electrolyte-side* is kept under air. In this case the biocathode behaves as a standard non-breathing electrode and the reduction current density is higher, ca 210 μA cm^{-2}. This is somewhat higher than expected, which probably means there is still some oxygen diffusion from the *gas-side*. Curve c) was started in the presence of argon but at the potential ca 0.45 V (forward cycle) the Ar flow to the *gas-side* of the cell was stopped and the air is allowed to enter. After changing of the gas the current density increased up to almost 1.50 mA cm^{-2} at 0.1 V. That indicates the sensitivity of the electrode to the concentration of dioxygen. Moreover the increase of the current density was immediate which indicates that the diffusion of gas through the Toray paper is very fast. The fourth scan (Fig. 3d)) shows the maximum current density which can be obtained with the presented biocathode – 2.15 mA cm^{-2} at 0.1 V. The value is consistent with the maximum limiting current determined for a similar catalytic layer on glassy carbon using rotating disk voltammetry [26]. To the best of our knowledge this is the highest

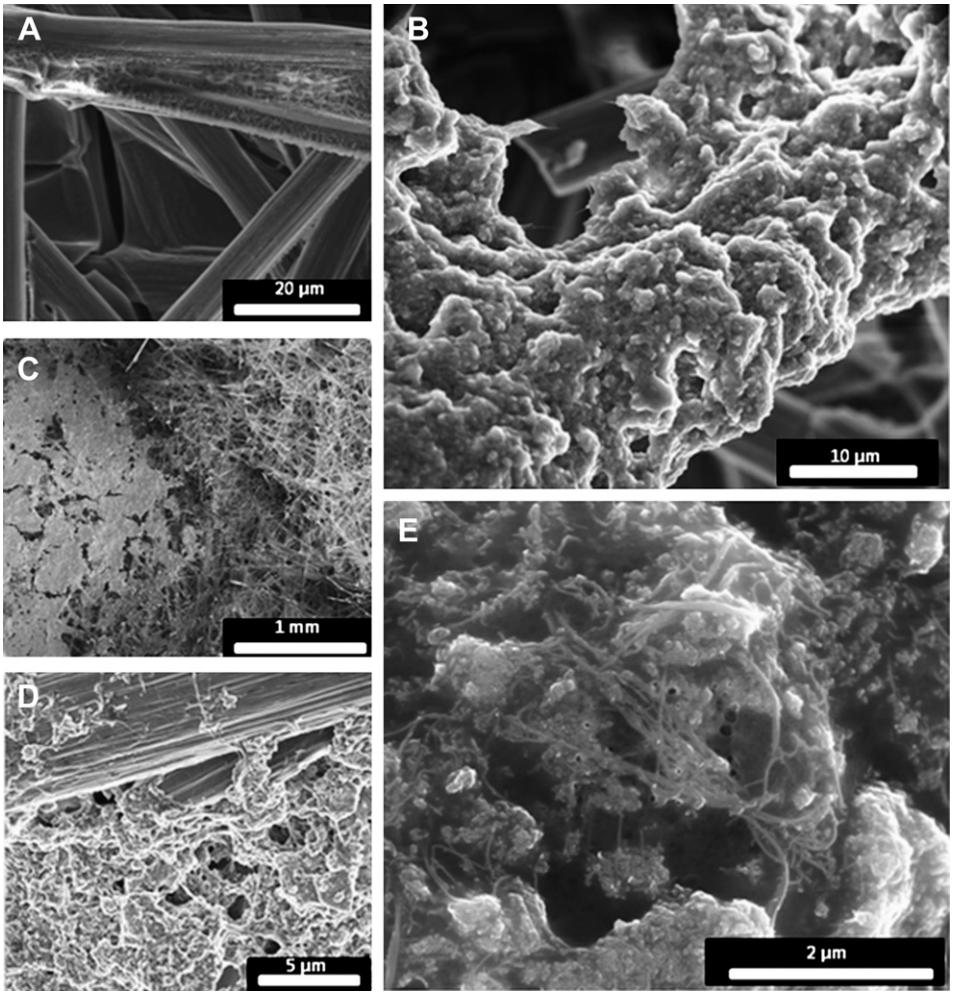

Fig. 2. SEM images of: Teflon treated Toray paper A) and the same paper modified with a porous silicate matrix in which enzyme and CNTs are encapsulated B), C), D) and E).

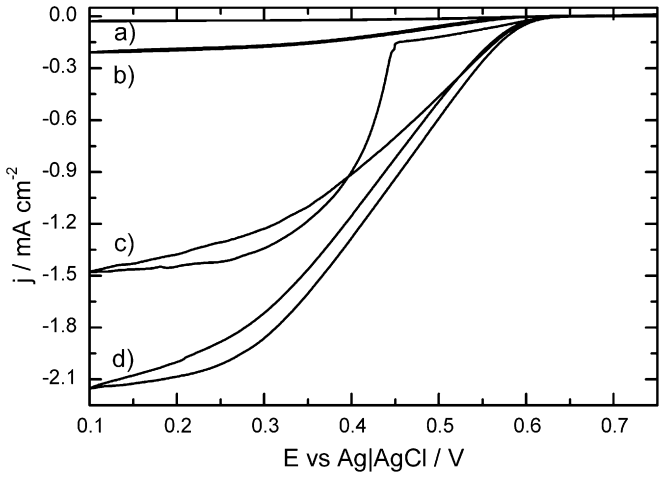

Fig. 3. Cyclic voltammetry (McIlvaine's buffer under air, pH = 4.8, v = 1 mV s^{-1}): oxygen reduction current with gases introduced to the *gas-side* as follows: argon b), air c) and dioxygen d). CV curve a) correspond to the situation where argon is introduced from the *gas-side*, while the electrolyte is also deaerated.

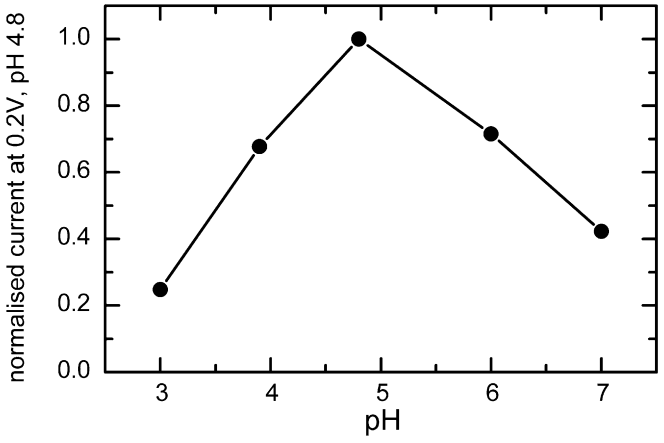

Fig. 4. pH dependance of dioxygen reduction current normalised to the current obtained for the air-breathing electrode in McIlvaine's buffer pH = 4.8. All data points were obtained from the current measured at potential 0.2 V vs. Ag|AgCl reference electrode (scan rate 1 mV s^{-1}).

current density of dioxygen reduction published so far using non-mediated systems with bilirubin oxidase.

Fig. 4 presents the pH dependance of dioxygen reduction on the air-breathing biocathode. All the measurements were performed in

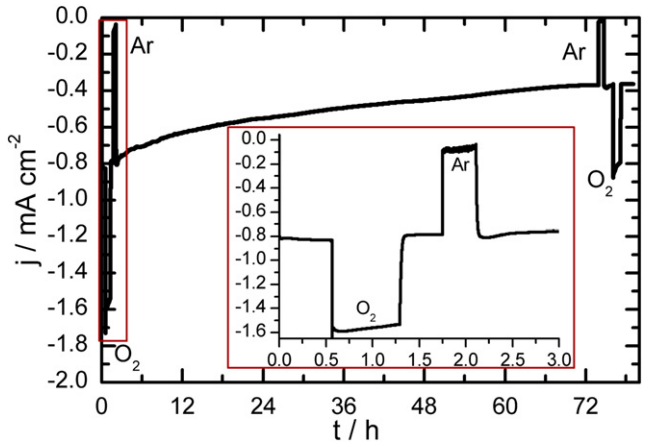

Fig. 6. Chronoamperometry of the air-breathing biocathode done in McIlvaine's buffer, pH = 4.8. The applied potential was 0.2 V vs. Ag|AgCl. The inset graph shows the first 3 h of the presented chronoamperogram.

0.1 M McIlvaine's buffer as an electrolyte. The current was measured with the gas-side exposed air. The cell performance was measured using CV and the current at 0.2 V vs. Ag|AgCl was plotted in the figure. The current value was normalised to the current obtained in pH = 4.8. The best performance of the electrode was noted for pH close to 5. This result is consistent with previously reported results [8,26].

3.3. Influence of the film composition on the performance of the biocathode

Electrodes with different material compositions were prepared to show their influence on the efficiency of the catalytic reduction of dioxygen. No oxygen reduction was observed on the Toray paper modified only with PTSA–SWCNT/$MTMOS_{gel}$ (Fig. 5a) in the scan range 0.75–0.1 V. This result was expected due to the lack of enzyme on the surface of the electrode. In the presence of BOD but the absence of PTSA–SWCNT (BOD/$MTMOS_{gel}$ electrode) a very low reduction current is noticed, ca 10 μA cm^{-2} at 0.1 V (Fig. 5b)). These results show that although the Toray paper itself can provide some contact with the enzyme the composite material need to encapsulate the enzyme together with the functionalised carbon nanotubes to give the best efficiency of dioxygen reduction (Fig. 5c)). Moreover, it is important to ensure that this material is properly dispersed on the Toray paper to give satisfactory results. Fig. 5d) shows a much lower current density on the PTSA–SWCNT/

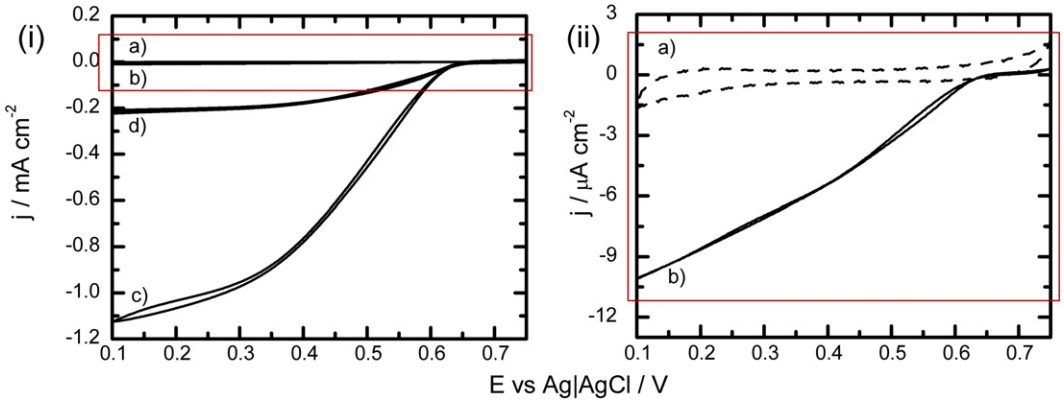

Fig. 5. Cyclic voltammetry of dioxygen reduction on the electrodes modified with $MTMOS_{gel}$ and: a) PTSA–SWCNT, b) BOD, c) and d) PTSA/SWCNT and BOD. In the case of d) CNTs with the enzyme formed a very compact layer on the Toray paper. McIlvaine's buffer, pH = 4.8, v = 1 mV s^{-1}, air. (ii) Is the scaled up version of (i).

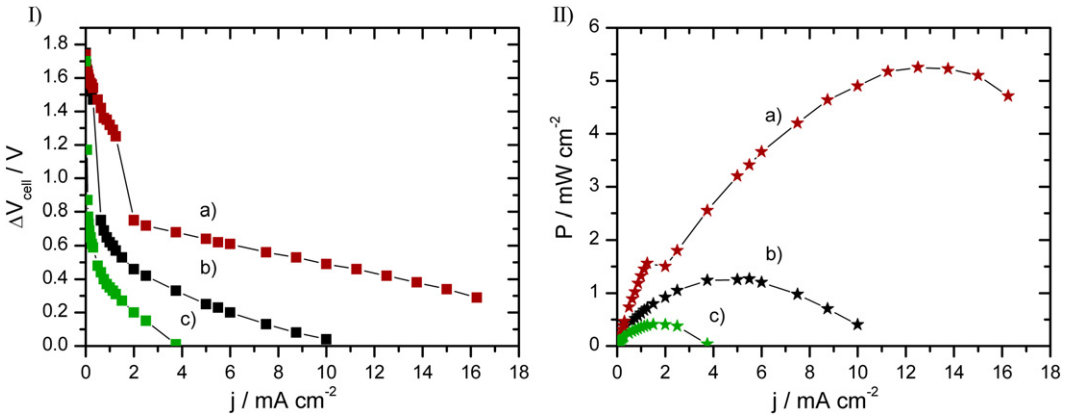

Fig. 7. (I) Galvanostatic polarisation curves and (II) the dependences of the power output for the zinc–oxygen biobattery with the electrolyte-side filled with McIlvaine's buffer, pH = 4.8 and the gas-side filled with: a) oxygen, b) air or c) argon.

BOD/MTMOS$_{gel}$ electrode in comparison with Fig. 5c). This effect was caused by the formation of a very compact layer of the composite which happens when a sol droplet is allowed to dry undisturbed on the hydrophobic surface of the Toray paper. To obtain better performing biocathodes (Fig. 5c)) the SWCNTs need to be mechanically spread out over the whole electrode surface prior to solvent evaporation and gelling. This observation is in agreement with the results published by Tarasevich et al. where more dispersed carbon nanomaterial improved direct electron transfer between the electrode and the active centre of laccase [13].

The stability of our biocathode was checked by conducting chronoamperometry with the applied voltage 0.2 V vs. Ag|AgCl for almost 80 h, mostly in air (Fig. 6). After that time the activity of the WE towards oxygen reduction was approximately half of that at the beginning. Moreover, chronoamperometry showed that the change of the gas into argon or oxygen caused very fast and pronounced change in the reduction current. Under argon flow the biocathode gave a negligible current whereas under oxygen flow the reduction current increased almost two times in comparison with keeping the *gas-side* in air.

3.4. Electrochemical characterisation of zinc/oxygen biobatteries

The construction of the zinc/oxygen battery was almost the same as shown in Fig. 1C). The only difference was that the RE and CE were replaced by the zinc anode.

Chronopotentiometry was used for measuring the polarisation curves for our battery. Different current loadings were applied in steps via the potentiostat and the voltage was measured as a response after reaching a stable value. The obtained polarisation curves showed that the open circuit voltage (OCV) was 1.75 V (Fig. 7), which is close to the theoretical value (1.99 V). This result is almost the same as the highest OCP published so far for biobatteries with carbon nanotubes (1.76 V) [27,28]. The power densities were also very high and highly dependent on the type of the gas introduced to the *gas-side*. The maximum power density of our

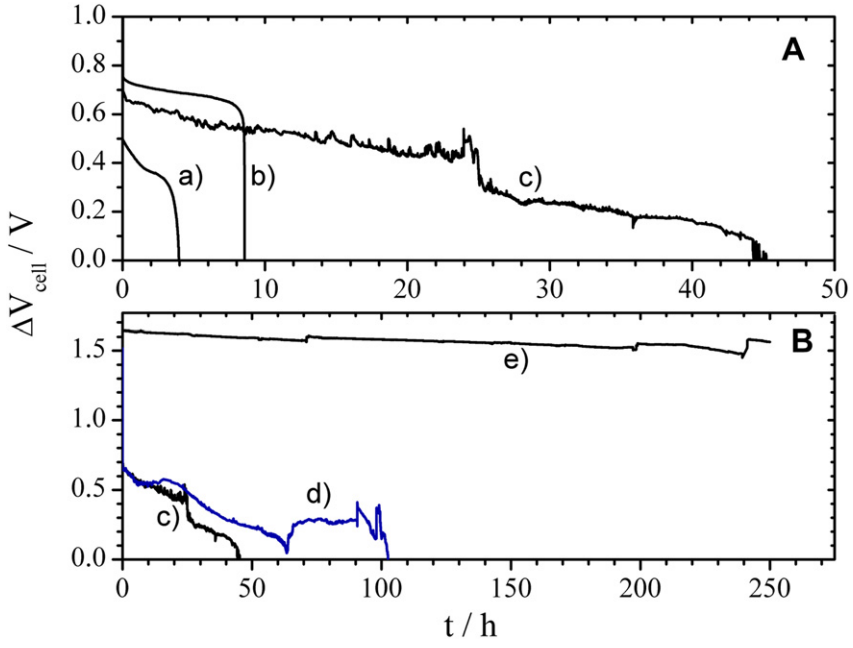

Fig. 8. Long term stability of the batteries checked with chronopotentiometry: A) curve a) −1250 μA cm^{-2}; b), c) −250 μA cm^{-2}, B) curve d) −250 μA cm^{-2}, e) −50 μA cm^{-2}, curve c) is the same as in A) The *gas-side* was filled with air and the *electrolyte-side* with: a), b) and e) McIlvaine's buffer, pH = 4.8, c) and d) phosphate buffer, pH = 7.0. The amount of enzyme on biocathode d) was twice that of biocathodes a), b), c) and e). Due to evaporation additional electrolyte was added after 71, 197 and 240 h (curve e).

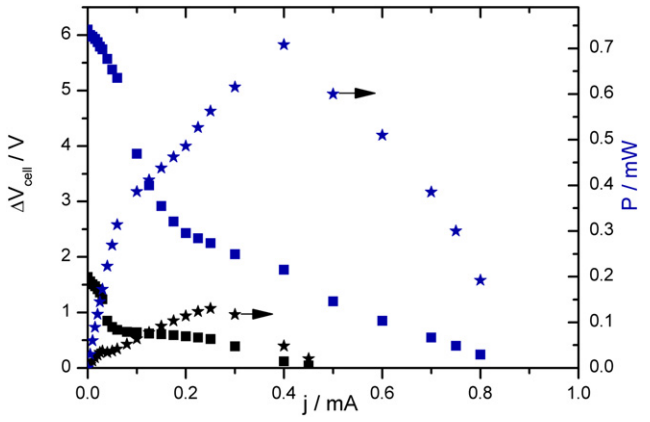

Fig. 9. Galvanostatic polarisation curves (squares) and the dependences of the power output (stars) for one (black) and a stack of four (blue) zinc/oxygen biobatteries. The *electrolyte-side* was filled with McIlvaine's buffer, pH = 4.8 and the *gas-side* was exposed to air. (For interpretation of the references to colour in this figure legend, the reader is referred to the web version of this article.)

biobattery working under oxygen in the *gas-side* was ca 5 times higher than in the case when this part of the battery was filled with the air. This dependance between the concentration of oxygen and the maximum power density indicates that the dioxygen reduction reaction in our biocathodes is very efficient.

Chronopotentiometry done under very high current load (−1250 μA cm^{-2}, Fig. 8A curve a) showed that our battery can operate for 4 h in McIlvaine's buffer, pH 4.8, the cell potential gradually decreasing. Under lower load (250 μA cm^{-2}, Fig. 8A curve b, and Fig. 8B curves c and d) the lifetime of the battery was longer and it reached almost 9 h in the same buffer. The gradual decrease of the voltage is caused by loss of catalytic activity of the cathode, as seen in Fig. 6. The sudden drop at the end of the battery lifetime is likely due to sudden failure of the Zn-anode. This behaviour closely matches observations by Shin et al. [25]. Changing the buffer to phosphate buffer at pH 7 increases the lifetime of the battery 5-fold. A further doubling of the lifetime could be achieved by doubling the amount of enzyme on the surface. In all cases the slope of the initial gradual decrease is the same as in McIlvaine's buffer. This supports the assumption that the rapid breakdown is due to the anode. However, if the load is kept at a moderate 50 μA cm^{-2} the lifetime of the battery is increased dramatically (Fig. 8B curve e). After 250 h the cell potential has decreased only 10%. This is in agreement with similar behaviour observed by Shleev et al. [14] also seeing a dramatic decrease in cathode lifetime under high load. The observation that an increase of the enzyme loading on the electrode or a decrease of the total current load prolongs the lifetime of the cathode supports the theory that a too high turnover rate for an individual enzyme leads to loss of catalytic activity.

To show that our battery can be used to power useful devices we connected it to a small clock (Fig. 2 in the supplementary material). The clock was working for at least 6 h.

For powering devices which need higher voltages one can make a stack of batteries connected in series. We connected 4 batteries in this way to obtain a source of power for a bike lamp composed of two red LEDs (Fig. 3 in the supplementary material). Galvanostatic polarisation curves and the dependences of the power output for 1 and 4 batteries from the stack are shown in Fig. 9 and were obtained in the same way as for the single cell. These results show that by connecting our batteries in series a relatively small footprint stack can deliver useful voltage for driving devices. The OCP increased by 1.5 V for each additional cell, showing the reproducibility of the assembly. Moreover, the power output increased drastically after connecting four batteries.

4. Conclusions

We have presented a simple method of fabricating efficient air-breathing biocathodes that can be assembled to zinc/oxygen batteries by connecting them with a properly pretreated zinc anode. Typically, in non-breathing biocathodes, the limiting step of the reaction is the depletion of the fuel in the vicinity of the catalytic layer. Here we avoid this problem by the construction of a breathing electrode. The breathing biocathode gives an oxygen reduction current of 1.5 mA cm^{-2} under air and over 2 mA cm^{-2} when breathing pure oxygen. The maximum power density of our zinc/oxygen battery breathing with oxygen showed in this paper was 5.25 mW cm^{-2} at ca 0.4 V, which is the best result published so far for such a device. Work is needed to improve the long term stability of both the anode and the biocathode.

A new design of a stack of four batteries let us obtain an energy source capable of powering a bike lamp with two LEDs.

Acknowledgements

This work was partially financed by The Polish Ministry of Science and Higher Education under the contract IP2011 020771. The work of AZ was realized within the International PhD Projects Programme of the Foundation for Polish Science, cofinanced from the European Regional Development Fund within the Innovative Economy Operational Programme "Grants for innovation". Access to SEM was realised by the EC 7. FP under the Research Potential (Coordination and Support Actions) (FP7-REGPOT-CT-2011-285949-NOBLESSE) project.

The authors thank Amano Enzyme Europe Ltd for the donation of bilirubin oxidase.

Appendix A. Supplementary data

Supplementary data related to this article can be found at http://dx.doi.org/10.1016/j.jpowsour.2012.11.081.

References

[1] A. Heller, Phys. Chem. Chem. Phys. 6 (2004) 206.
[2] H. Sakai, T. Nakagawa, Y. Tokita, T. Hatazawa, T. Ikeda, S. Tsujimura, K. Kano, Energy Environ. Sci. 2 (2009) 133.
[3] A. Wieckowski, J. Norskow (Eds.), Fuel Cell Science: Theory, Fundamentals And Biocatalysis, John Wiley & Sons, Hoboken, New Jersey, 2010.
[4] E.I. Solomon, U.M. Sundaram, T.E. Machonkin, Chem. Rev. 96 (1996) 2563.
[5] S. Tsujimura, K. Kano, T. Ikeda, J. Electroanal. Chem. 576 (2005) 113.
[6] P. Ramírez, N. Mano, R. Andreu, T. Ruzgas, A. Heller, L. Gorton, S. Shleev, Biochim. Biophys. Acta 1777 (2008) 1364.
[7] S. Shleev, M. Klis, Y. Wang, J. Rogalski, R. Bilewicz, L. Gorton, Electroanalysis 19 (2007) 1039.
[8] V. Coman, R. Ludwig, W. Harreither, D. Haltrich, L. Gorton, T. Ruzgas, S. Shleev, Fuel Cells 10 (2010) 9.
[9] T. Miyake, K. Haneda, N. Nagai, Y. Yatagawa, H. Onami, S. Yoshino, T. Abe, M. Nishizawa, Energy Environ. Sci. 4 (2011) 5008.
[10] S.C. Barton, Electrochim. Acta 50 (2005) 2145.
[11] K.G. Lim, G.T.R. Palmore, Biosens. Bioelectron. 22 (2007) 941.
[12] A. Zebda, C. Innocent, L. Renaud, M. Cretin, F. Pichot, R. Ferrigno, S. Tingry, Enzyme-Based Microfluidic Biofuel Cell To Generate Micropower, in: M.A. dos Santos Bernardes (Ed.), Biofuel's Engineering Process Technology, InTech, 2011.
[13] M.R. Tarasevich, V.A. Bogdanovskaya, A.V. Kapustin, Electrochem. Commun. 5 (2003) 491.
[14] S. Shleev, G. Shumakovich, O. Morozova, A. Yaropolov, Fuel Cells 4 (2010) 726.
[15] W. Nogala, A. Celebanska, G. Wittstock, M. Opallo, Fuel Cells 10 (2010) 1157.
[16] R. Kontani, S. Tsujimura, K. Kano, Bioelectrochemistry 76 (2009) 10.
[17] R.A. Rincón, C. Lau, H.R. Luckarift, K.E. Garcia, E. Adkins, G.R. Johnson, P. Atanassov, Biosens. Bioelectron. 27 (2011) 132.
[18] G. Gupta, C. Lau, B. Branch, V. Rajendran, D. Ivnitski, P. Atanassov, Electrochim. Acta 56 (2011) 10767.
[19] G. Gupta, C. Lau, V. Rajendran, F. Colon, B. Branch, D. Ivnitski, P. Atanassov, Electrochem. Commun. 13 (2011) 247.
[20] C. Lau, E.R. Adkins, R.P. Ramasamy, H.R. Luckarift, G.R. Johnson, P. Atanassov, Adv. Energy Mater. 2 (2012) 162.

[21] W. Gellett, J. Schumacher, M. Kesmez, D. Le, S.D. Minteer, J. Electrochem. Soc. 157 (2010) B557.
[22] M. Jönsson-Niedziolka, K. Szot, J. Rogalski, M. Opallo, Electrochem. Commun. 11 (2009) 1042.
[23] K. Szot, J. Niedziolka, J. Rogalski, F. Marken, M. Opallo, J. Electroanal. Chem. 612 (2008) 1.
[24] I. Zawisza, J. Rogalski, M. Opallo, J. Electroanal. Chem. 588 (2006) 244.
[25] W. Shin, J. Lee, Y. Kim, H. Steinfink, A. Heller, J. Am. Chem. Soc. 127 (2005) 14590.
[26] M. Jönsson-Niedziolka, A. Kaminska, M. Opallo, Electrochim. Acta 55 (2010) 8744.
[27] U.B. Jensen, S. Lörcher, M. Vagin, J. Chevallier, S. Shipovskov, O. Koroleva, F. Besenbacher, E.E. Ferapontova, Electrochim. Acta 62 (2012) 218.
[28] M. Holzinger, A. Le Goff, S. Cosnier, Electrochim. Acta 82 (2012) 179–190.